THREE-DIMENSIONAL SOLUTION FOR THE STRESS FIELD AROUND A CIRCULAR HOLE IN A PLATE

W.-D. Tseng *

Department of Construction Engineering
Nan Jeon University of Science and Technology
Tainan, Taiwan

J.-Q. Tarn

Department of Civil Engineering
National Cheng Kung University
Tainan, Taiwan

ABSTRACT

We present an exact analysis of the stress field around a circular hole in an elastic plate under remote loading. On the basis of Hamiltonian state space approach, a rigorous 3D solution of the problem is determined in a systematic way by means of separation of variables and symplectic eigenfunction expansion, thereby, the thickness effect on stress concentration around the circular hole and the applicability of the classical 2D solution for the problem are evaluated.

Keywords: Circular hole, Hamiltonian, State space, Stress concentration, Three-dimensional elasticity.

1. INTRODUCTION

Stress concentration around a hole in an elastic medium has been studied extensively under the plane strain or plane stress assumptions [1,2], but rarely in 3D. It is well known that the plane-strain state occurs in a long cylindrical body of uniform cross-section subjected to axially invariant loads; whereas the plane stress state occurs in a thin plate subjected to inplane loads. When the plate thickness is comparable with the dimension of the hole, the stress field near the hole is inherently 3D. To assess the applicability of the 2D solution for the problem, it is necessary to conduct a rigorous 3D analysis.

Exact analysis of the stress field in a notched plate of arbitrary thickness is difficult. A number of solutions considering the thickness effect can be found in the literature, ranging from analytic solutions based on simplifying assumptions [3] to numerical solutions using the finite element codes [4-6]. Folias and Wang [7] presented a complicated solution for evaluating the stresses around a circular hole subjected to remote tensile load. Their analysis is based on a series solution to Navier's equations for a plate of uniform thickness [8] in which the unknown constants are computed from the boundary conditions at the hole by using an approximate method [9]. They concluded that the 3D stress concentration factor is only slightly different from the 2D one over a wide range of the radius to thickness ratio a/h.

Recently, we have developed a Hamiltonian state space formalism and solution approach to anisotropic elasticity and applied it to various classes of problems [10-14]. Here we present an exact 3D analysis of stress field in an elastic plate containing a circular hole under remote loading. The plate is considered to be transversely isotropic with isotropy as a special case. On the basis of Hamiltonian state space formulation, the basic equations of elasticity in cylindrical coordinates are formulated into a state equation and an output equation in terms of the state vector composed of the displacement vector and the conjugate stress vector as the dual variables. A salient feature of the formulation is that it brings out the Hamiltonian characteristics of the problem such that the state equation exhibits Hamiltonian features and the associated eigensystem possesses symplectic orthogonality, which provide an essential basis for using eigenfunction expansion to determine the 3D solution of the problem.

In this paper we first revisit the 2D solution for the problem by the state space approach and then derive the 3D solution. In the state space setting, solving the state equation under the traction-free boundary conditions at the top and bottom surfaces of the plate gives rise to a Hamiltonian eigensystem. It is shown that the eigenvalues μ of the system appear in positive and negative pairs $(\mu, -\mu)$ and $\mu = 0$ is a repeated eigenvalue. Furthermore, the eigenvectors possess symplectic orthogonality. Upon deriving the linearly independent eigenvectors associated with all the eigenvalues, a linear combination of the eigensolutions yields a 3D series solution for the problem. The remaining task of determining the constants of linear combination so as to satisfy the traction-free conditions on the hole boundary at $r = a$ and the loading conditions at $r \to \infty$ is accomplished by means of symplectic eigenfunction expansion in a systematic way. In the light of the present 3D solution, we are able to evaluate the thickness effect on the stress concentration around the circular hole and the applicability of the 2D solution.

* Corresponding author (wdtseng@mail.nju.edu.tw)

DOI : 10.1017/jmech.2014.48
Copyright © 2014 The Society of Theoretical and Applied Mechanics, R.O.C.
https://doi.org/10.1017/jmech.2014.48 Published online by Cambridge University Press

2. PROBLEM STATEMENT

Consider an elastic plate of arbitrary thickness $2h$ containing a circular hole subjected to remote loading as in Fig. 1. Let us locate the origin of the cylindrical coordinates (r, θ, z) at the center of the circular hole. With z axis being the axis of symmetry, the constitutive equations of transversely isotropic elastic materials are

$$\begin{bmatrix} \sigma_{rr} \\ \sigma_{\theta\theta} \\ \sigma_{zz} \\ \sigma_{\theta z} \\ \sigma_{rz} \\ \sigma_{r\theta} \end{bmatrix} = \begin{bmatrix} c_{11} & c_{12} & c_{13} & 0 & 0 & 0 \\ c_{12} & c_{11} & c_{13} & 0 & 0 & 0 \\ c_{13} & c_{13} & c_{33} & 0 & 0 & 0 \\ 0 & 0 & 0 & c_{44} & 0 & 0 \\ 0 & 0 & 0 & 0 & c_{44} & 0 \\ 0 & 0 & 0 & 0 & 0 & c_{66} \end{bmatrix} \begin{bmatrix} \varepsilon_{rr} \\ \varepsilon_{\theta\theta} \\ \varepsilon_{zz} \\ 2\varepsilon_{\theta z} \\ 2\varepsilon_{rz} \\ 2\varepsilon_{r\theta} \end{bmatrix}, \tag{1}$$

where, it is understood that the indices 1, 2, 3 stand for r, θ and z, respectively; σ_{ij} and ε_{ij} are the stress and strain components; c_{ij} are the elastic constants, and $c_{66} = (c_{11} - c_{12})/2$. With $c_{33} = c_{11}$, $c_{13} = c_{12}$, and $c_{44} = c_{66} = (c_{11} - c_{12})/2$, the independent elastic constants reduce from five to two for isotropic materials.

The strain-displacement relations are

$$\varepsilon_{rr} = \frac{\partial u_r}{\partial r}, \quad \varepsilon_{\theta\theta} = \frac{1}{r}\frac{\partial u_\theta}{\partial \theta} + \frac{u_r}{r}, \quad \varepsilon_{zz} = \frac{\partial u_z}{\partial z},$$
$$\varepsilon_{\theta z} = \frac{1}{2}\left(\frac{\partial u_\theta}{\partial z} + \frac{1}{r}\frac{\partial u_z}{\partial \theta}\right), \quad \varepsilon_{rz} = \frac{1}{2}\left(\frac{\partial u_z}{\partial r} + \frac{\partial u_r}{\partial z}\right),$$
$$\varepsilon_{r\theta} = \frac{1}{2}\left(\frac{1}{r}\frac{\partial u_r}{\partial \theta} + \frac{\partial u_\theta}{\partial r} - \frac{u_\theta}{r}\right). \tag{2}$$

The equilibrium equations in the absence of the body force are

$$\frac{\partial \sigma_{rr}}{\partial r} + \frac{1}{r}\frac{\partial \sigma_{r\theta}}{\partial \theta} + \frac{\partial \sigma_{rz}}{\partial z} + \frac{\sigma_{rr} - \sigma_{\theta\theta}}{r} = 0,$$
$$\frac{\partial \sigma_{r\theta}}{\partial r} + \frac{1}{r}\frac{\partial \sigma_{\theta\theta}}{\partial \theta} + \frac{\partial \sigma_{\theta z}}{\partial z} + \frac{2\sigma_{r\theta}}{r} = 0,$$
$$\frac{\partial \sigma_{rz}}{\partial r} + \frac{1}{r}\frac{\partial \sigma_{\theta z}}{\partial \theta} + \frac{\partial \sigma_{zz}}{\partial z} + \frac{\sigma_{rz}}{r} = 0, \tag{3}$$

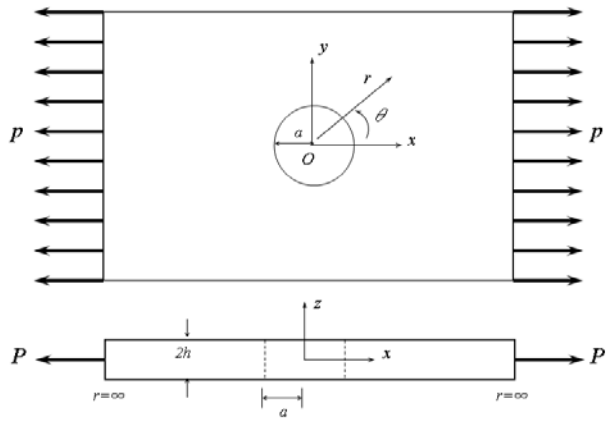


Fig. 1 An elastic plate with a circular hole under remote extension.

On the basis of the Hamiltonian state space formulation for anisotropic elasticity [10,13], by taking the displacement vector $[u_r, u_\theta, u_z]$ and the conjugate stress vector $[r\sigma_{rr}, r\sigma_{r\theta}, r\sigma_{rz}]$ to form the state vector, Eqs. (1) ~ (3) can be expressed into a state equation and an output equation as follows:

$$r\frac{\partial}{\partial r}\begin{bmatrix} u_r \\ u_\theta \\ u_z \\ r\sigma_{rr} \\ r\sigma_{r\theta} \\ r\sigma_{rz} \end{bmatrix} = \begin{bmatrix} -\hat{c}_{12} & -\hat{c}_{12}\partial_\theta & -\hat{c}_{13} r\partial_z & c_{11}^{-1} & 0 & 0 \\ -\partial_\theta & 1 & 0 & 0 & c_{66}^{-1} & 0 \\ -r\partial_z & 0 & 0 & 0 & 0 & c_{44}^{-1} \\ \tilde{c}_{22} & \tilde{c}_{22}\partial_\theta & \tilde{c}_{23} r\partial_z & \hat{c}_{12} & -\partial_\theta & -r\partial_z \\ -\tilde{c}_{22}\partial_\theta & l_{52} & l_{53} & -\hat{c}_{12}\partial_\theta & -1 & 0 \\ -\tilde{c}_{23} r\partial_z & l_{53} & l_{63} & -\hat{c}_{13} r\partial_z & 0 & 0 \end{bmatrix} \begin{bmatrix} u_r \\ u_\theta \\ u_z \\ r\sigma_{rr} \\ r\sigma_{r\theta} \\ r\sigma_{rz} \end{bmatrix}, \tag{4}$$

$$\begin{bmatrix} r\sigma_{\theta\theta} \\ r\sigma_{\theta z} \\ r\sigma_{zz} \end{bmatrix} = \begin{bmatrix} \tilde{c}_{22} & \tilde{c}_{22}\partial_\theta & \tilde{c}_{23} r\partial_z & \hat{c}_{12} \\ 0 & c_{44} r\partial_z & c_{44}\partial_\theta & 0 \\ \tilde{c}_{23} & \tilde{c}_{23}\partial_\theta & \tilde{c}_{33} r\partial_z & \hat{c}_{13} \end{bmatrix} \begin{bmatrix} u_r \\ u_\theta \\ u_z \\ r\sigma_{rr} \end{bmatrix}, \tag{5}$$

where ∂_r, ∂_θ and ∂_z denote partial differentiation with respect to r, θ and z, respectively, and

$$\hat{c}_{ij} = c_{ij} c_{11}^{-1}, \quad \tilde{c}_{ij} = c_{ij} - c_{i1} c_{11}^{-1} c_{j1},$$
$$l_{52} = -(\tilde{c}_{22}\partial_{\theta\theta} + c_{44} r^2 \partial_{zz}), \quad l_{53} = -(\tilde{c}_{23} + c_{44}) r\partial_{\theta z},$$
$$l_{63} = -(c_{44}\partial_{\theta\theta} + \tilde{c}_{33} r^2 \partial_{zz}).$$

In case the radius a of the circular hole is small relative to the inplane dimensions of the plate, the loading condition for the plate subjected to remote inplane loads is

$$[\sigma_{rr} \ \ \sigma_{r\theta} \ \ \sigma_{rz}]_{r\to\infty} = [p_1(\theta) \ \ p_2(\theta) \ \ 0], \tag{6}$$

where $P_i(\theta)$ are prescribed functions of θ. Specifically, the loading condition for the plate subjected to remote extension P in x direction is

$$[\sigma_{rr} \ \ \sigma_{r\theta} \ \ \sigma_{rz}]_{r\to\infty} = \left[\frac{p}{2}(1+\cos 2\theta) \ \ -\frac{p}{2}\sin 2\theta \ \ 0\right]. \tag{7}$$

The circular hole boundary and the top and bottom surfaces of the plate are traction-free so that the boundary conditions at $r = a$ and at $z = \pm h$ are

$$[\sigma_{rr} \ \ \sigma_{r\theta} \ \ \sigma_{rz}]_{r=a} = [0 \ \ 0 \ \ 0], \tag{8}$$

$$[\sigma_{rz} \ \ \sigma_{\theta z} \ \ \sigma_{zz}]_{z=\pm h} = [0 \ \ 0 \ \ 0]. \tag{9}$$

Given the state space formulation of the problem, our task is to solve the state equation Eq. (4) under the boundary conditions Eqs. (6) ~ (9). Once the state vector is determined, the remaining unknown stress components are derived from the output equation.

https://doi.org/10.1017/jmech.2014.48 Published online by Cambridge University Press

3. TWO-DIMENSIONAL SOLUTION

First, let us revisit the 2D solution of the problem in the present context. When the displacement and stress fields are independent of z, the state equation and the output equation are decoupled into two sets of equations. One for the inplane deformation:

$$r\frac{\partial}{\partial r}\begin{bmatrix} u_r \\ u_\theta \\ r\sigma_{rr} \\ r\sigma_{r\theta} \end{bmatrix} = \begin{bmatrix} -\hat{c}_{12} & -\hat{c}_{12}\partial_\theta & c_{11}^{-1} & 0 \\ -\partial_\theta & 1 & 0 & c_{66}^{-1} \\ \tilde{c}_{22} & \tilde{c}_{22}\partial_\theta & \hat{c}_{12} & -\partial_\theta \\ -\tilde{c}_{22}\partial_\theta & -\tilde{c}_{22}\partial_{\theta\theta} & -\hat{c}_{12}\partial_\theta & -1 \end{bmatrix} \begin{bmatrix} u_r \\ u_\theta \\ r\sigma_{rr} \\ r\sigma_{r\theta} \end{bmatrix}, \tag{10}$$

$$\begin{bmatrix} r\sigma_{\theta\theta} \\ r\sigma_{zz} \end{bmatrix} = \begin{bmatrix} \tilde{c}_{22} & \tilde{c}_{22}\partial_\theta & \hat{c}_{12} \\ \tilde{c}_{23} & \tilde{c}_{23}\partial_\theta & \hat{c}_{13} \end{bmatrix} \begin{bmatrix} u_r \\ u_\theta \\ r\sigma_{rr} \end{bmatrix}, \tag{11}$$

the other for the antiplane deformation:

$$r\frac{\partial}{\partial r}\begin{bmatrix} u_z \\ r\sigma_{rz} \end{bmatrix} = \begin{bmatrix} 0 & c_{44}^{-1} \\ -c_{44}\partial_{\theta\theta} & 0 \end{bmatrix} \begin{bmatrix} u_z \\ r\sigma_{rz} \end{bmatrix}, \tag{12}$$

$$r\sigma_{\theta z} = c_{44}\frac{\partial u_z}{\partial \theta}. \tag{13}$$

The solution to Eqs. (12) ~ (13) under the BC Eqs. (6) ~ (8) is trivial ($u_z = \sigma_{rz} = \sigma_{\theta z} = 0$), so it suffices to solve Eq. (10) under the associated boundary conditions. To this end, we express the solution of Eq. (10) in the form of the Fourier series:

$$[u_r \;\; u_\theta \;\; r\sigma_{rr} \;\; r\sigma_{r\theta}] = \sum_{n=-\infty}^{\infty} [U(r) \;\; V(r) \;\; X(r) \;\; Y(r)]_n e^{in\theta}, \tag{14}$$

where $U_n(r)$, $V_n(r)$, $X_n(r)$, and $Y_n(r)$ are unknown functions of r.

Substituting Eq. (14) in Eq. (10) gives

$$r\frac{d}{dr}\begin{bmatrix} U \\ V \\ X \\ Y \end{bmatrix}_n = \begin{bmatrix} -\hat{c}_{12} & -in\hat{c}_{12} & c_{11}^{-1} & 0 \\ -in & 1 & 0 & c_{66}^{-1} \\ \tilde{c}_{22} & in\tilde{c}_{22} & \hat{c}_{12} & -in \\ -in\tilde{c}_{22} & n^2\tilde{c}_{22} & -in\hat{c}_{12} & -1 \end{bmatrix} \begin{bmatrix} U \\ V \\ X \\ Y \end{bmatrix}_n, \tag{15}$$

By letting

$$[U \;\; V \;\; X \;\; Y]_n = r^{\lambda_n}[c_1 \;\; c_2 \;\; c_3 \;\; c_4]_n, \tag{16}$$

where λ_n and c_1, c_2, c_3, c_4 are unknown parameters and constant coefficients to be determined, Eq. (15) reduces to

$$\begin{bmatrix} -\hat{c}_{12}-\lambda_n & -in\hat{c}_{12} & c_{11}^{-1} & 0 \\ -in & 1-\lambda_n & 0 & c_{66}^{-1} \\ \tilde{c}_{22} & in\tilde{c}_{22} & \hat{c}_{12}-\lambda_n & -in \\ -in\tilde{c}_{22} & n^2\tilde{c}_{22} & -in\hat{c}_{12} & -1-\lambda_n \end{bmatrix} \begin{bmatrix} c_1 \\ c_2 \\ c_3 \\ c_4 \end{bmatrix}_n = \begin{bmatrix} 0 \\ 0 \\ 0 \\ 0 \end{bmatrix}, \tag{17}$$

which has non-trivial solutions if the determinant of the coefficient matrix equals to zero. This condition yields 4 roots: $\lambda_{nk} = \pm(n+1), \pm(n-1)$. To each λ_{nk} there corresponds a solution of $[c_1, c_2, c_3, c_4]_{nk}$ determined within a constant multiplier.

There follows

$$[u_r \;\; u_\theta \;\; r\sigma_{rr} \;\; r\sigma_{r\theta}] = \sum_{n=-\infty}^{\infty}\sum_{k=1}^{4} A_{nk}\, r^{\lambda_{nk}} [c_1 \;\; c_2 \;\; c_3 \;\; c_4]_{nk} e^{in\theta}, \tag{18}$$

$$\begin{bmatrix} r\sigma_{\theta\theta} \\ r\sigma_{zz} \end{bmatrix} = \sum_{n=-\infty}^{\infty}\sum_{k=1}^{4} A_{nk}\, r^{\lambda_{nk}} \begin{bmatrix} \tilde{c}_{22} & in\tilde{c}_{22} & \hat{c}_{12} \\ \tilde{c}_{23} & in\tilde{c}_{23} & \hat{c}_{13} \end{bmatrix} \begin{bmatrix} c_1 \\ c_2 \\ c_3 \end{bmatrix}_{nk} e^{in\theta}, \tag{19}$$

where A_{nk} are constants to be determined by satisfying the inplane boundary conditions at $r = a$ and at $r \to \infty$.

Imposing the boundary conditions at $r \to \infty$ and at $r = a$ given by Eqs. (7) and (8) on the relevant stress components in Eqs. (18) ~ (19), determining A_{nk} by comparison of coefficients using

$$\cos 2\theta = (e^{-i2\theta} + e^{i2\theta})/2, \quad \sin 2\theta = i(e^{-i2\theta} - e^{i2\theta})/2, \tag{20}$$

we find that $A_{nk} \neq 0$ only when $n = 0, \pm 2$, and the two-dimensional solution for the problem of the plate subjected to remote tension p in the x direction is

$$u_z = \sigma_{rz} = \sigma_{\theta z} = 0, \tag{21}$$

$$\begin{bmatrix} u_r \\ u_\theta \end{bmatrix} = \frac{p}{2}\begin{bmatrix} \left(\frac{1}{c_{11}+c_{12}} + \frac{1}{c_{11}-c_{12}}\frac{a^2}{r^2}\right) r \\ + \frac{1}{c_{11}-c_{12}}\left(1 + \frac{4c_{11}}{c_{11}+c_{12}}\frac{a^2}{r^2} - \frac{a^4}{r^4}\right) r\cos 2\theta \\ -\left(\frac{1}{c_{11}-c_{12}} + \frac{2}{c_{11}+c_{12}}\frac{a^2}{r^2} + \frac{1}{c_{11}-c_{12}}\frac{a^4}{r^4}\right) r\sin 2\theta \end{bmatrix}, \tag{22}$$

$$\begin{bmatrix} \sigma_{rr} \\ \sigma_{r\theta} \\ \sigma_{\theta\theta} \\ \sigma_{zz} \end{bmatrix} = \frac{p}{2}\begin{bmatrix} \left(1-\frac{a^2}{r^2}\right)\left[1+\left(1-3\frac{a^2}{r^2}\right)\cos 2\theta\right] \\ -\left(1-\frac{a^2}{r^2}\right)\left(1+3\frac{a^2}{r^2}\right)\sin 2\theta \\ 1+\frac{a^2}{r^2}-\left(1+3\frac{a^4}{r^4}\right)\cos 2\theta \\ \frac{2c_{13}}{c_{11}+c_{12}}\left(1-2\frac{a^2}{r^2}\cos 2\theta\right) \end{bmatrix}. \tag{23}$$

The classical 2D solution [1] for isotropic materials is recovered by letting $c_{33} = c_{11}$, $c_{13} = c_{12}$, $c_{44} = c_{66} = (c_{11} - c_{12})/2$ in Eqs. (21) ~ (23). Such a solution does not satisfy the traction-free boundary conditions on the top and bottom surfaces.

https://doi.org/10.1017/jmech.2014.48 Published online by Cambridge University Press

4. THREE-DIMENSIONAL SOLUTION

To determine the three-dimensional solution for the problem, it is necessary to solve Eq. (4) under the boundary conditions given by Eqs. (6) ~ (9). To this end, let us express the solution of Eqs. (4) and (5) in the form of the Fourier series:

$$\begin{bmatrix} u_r \\ u_\theta \\ u_z \\ r\sigma_{rr} \\ r\sigma_{r\theta} \\ r\sigma_{rz} \end{bmatrix} = \sum_{n=-\infty}^{\infty} \begin{bmatrix} U_r(r,z) \\ U_\theta(r,z) \\ U_z(r,z) \\ S_{rr}(r,z) \\ S_{r\theta}(r,z) \\ S_{rz}(r,z) \end{bmatrix}_n e^{in\theta}, \qquad \begin{bmatrix} r\sigma_{\theta\theta} \\ r\sigma_{\theta z} \\ r\sigma_{zz} \end{bmatrix} = \sum_{n=-\infty}^{\infty} \begin{bmatrix} S_{\theta\theta}(r,z) \\ S_{\theta z}(r,z) \\ S_{zz}(r,z) \end{bmatrix}_n e^{in\theta}, \tag{24}$$

where $U_r(r, z)$, $U_\theta(r, z)$, $\cdots$, $S_{zz}(r, z)$ are unknown functions of r and z.

Substituting Eq. (24) into Eqs. (4) ~ (5) yields the equations for each harmonics of θ:

$$r\frac{\partial}{\partial r}\begin{bmatrix} U_r \\ U_\theta \\ U_z \\ S_{rr} \\ S_{r\theta} \\ S_{rz} \end{bmatrix}_n = \begin{bmatrix} -\hat{c}_{12} & -in\hat{c}_{12} & -\hat{c}_{13}\, r\partial_z & c_{11}^{-1} & 0 & 0 \\ -in & 1 & 0 & 0 & c_{66}^{-1} & 0 \\ -r\partial_z & 0 & 0 & 0 & 0 & c_{44}^{-1} \\ \tilde{c}_{22} & in\tilde{c}_{22} & \tilde{c}_{23}\, r\partial_z & \hat{c}_{12} & -in & -r\partial_z \\ -in\tilde{c}_{22} & d_{52} & d_{53} & -in\hat{c}_{12} & -1 & 0 \\ -\tilde{c}_{23}\, r\partial_z & d_{53} & d_{63} & -\hat{c}_{13} r\partial_z & 0 & 0 \end{bmatrix} \begin{bmatrix} U_r \\ U_\theta \\ U_z \\ S_{rr} \\ S_{r\theta} \\ S_{rz} \end{bmatrix}_n, \tag{25}$$

$$\begin{bmatrix} S_{\theta\theta} \\ S_{\theta z} \\ S_{zz} \end{bmatrix}_n = \begin{bmatrix} \tilde{c}_{22} & in\tilde{c}_{22} & \tilde{c}_{23}\, r\partial_z & \hat{c}_{12} \\ 0 & c_{44}\, r\partial_z & inc_{44} & 0 \\ \tilde{c}_{23} & in\tilde{c}_{23} & \tilde{c}_{33}\, r\partial_z & \hat{c}_{13} \end{bmatrix} \begin{bmatrix} U_r \\ U_\theta \\ U_z \\ S_{rr} \end{bmatrix}_n, \tag{26}$$

where

$$d_{52} = \tilde{c}_{22}n^2 - c_{44}r^2\partial_{zz}, \quad d_{53} = -in(\tilde{c}_{23} + c_{44})r\partial_z,$$
$$d_{63} = c_{44}n^2 - \tilde{c}_{33}r^2\partial_{zz}.$$

Guided by our experience with the problems in the cylindrical coordinate system [13], we seek the solution to Eq. (25) in the form

$$\begin{bmatrix} U_r \\ U_\theta \\ U_z \\ S_{rr} \\ S_{r\theta} \\ S_{rz} \end{bmatrix}_n = \begin{bmatrix} U_n\, K_{n-1}(\lambda r) + U_n' K_{n+1}(\lambda r) \\ V_n\, K_{n-1}(\lambda r) + V_n' K_{n+1}(\lambda r) \\ W_n\, K_n(\lambda r) \\ X_n\, rK_n(\lambda r) + X_n' K_{n-1}(\lambda r) + X_n'' K_{n+1}(\lambda r) \\ Y_n\, rK_n(\lambda r) + Y_n' K_{n-1}(\lambda r) + Y_n'' K_{n+1}(\lambda r) \\ Z_n'\, rK_{n-1}(\lambda r) + Z_n'' rK_{n+1}(\lambda r) \end{bmatrix}, \tag{27}$$

where U_r, U_n', V_n, V_n', W_n, $X_n, \cdots, Z_n'$ are unknown functions of z, $K_n(\lambda r)$ is the modified Bessel function of the second kind of order n, which is a monotonically decaying function, λ is an undetermined parameter.

Substituting Eq. (27) in Eq. (25), after manipulation using the derivative formulas of Bessel functions [15], we arrive at

$$\mathbf{H}\boldsymbol{\psi} = \lambda\boldsymbol{\psi}, \tag{28}$$

where

$$\mathbf{H} = \begin{bmatrix} \mathbf{L}_{11} & \mathbf{L}_{12} \\ \mathbf{L}_{21} & \mathbf{L}_{11}^* \end{bmatrix}, \quad \boldsymbol{\psi} = \begin{bmatrix} \mathbf{U}_n \\ r^{-1}\mathbf{S}_n \end{bmatrix},$$
$$\mathbf{U}_n = \begin{bmatrix} U_n' + U_n \\ V_n' + V_n \\ W_n \end{bmatrix}, \quad \mathbf{S}_n = \begin{bmatrix} X_n \\ Y_n \\ Z_n'' + Z_n' \end{bmatrix},$$

$$\mathbf{L}_{11} = \begin{bmatrix} 0 & 0 & -\hat{c}_{13}\, d_z \\ 0 & 0 & 0 \\ -d_z & 0 & 0 \end{bmatrix}, \quad \mathbf{L}_{11}^* = \begin{bmatrix} 0 & 0 & -d_z \\ 0 & 0 & 0 \\ -\hat{c}_{13}\, d_z & 0 & 0 \end{bmatrix},$$

$$\mathbf{L}_{12} = \begin{bmatrix} c_{11}^{-1} & 0 & 0 \\ 0 & c_{66}^{-1} & 0 \\ 0 & 0 & c_{44}^{-1} \end{bmatrix}, \quad \mathbf{L}_{21} = \begin{bmatrix} 0 & 0 & 0 \\ 0 & -c_{44}\, d_{zz} & 0 \\ 0 & 0 & -c_{33}\, d_{zz} \end{bmatrix},$$

$$V_n' - V_n = i(U_n' + U_n), \quad U_n' - U_n = -i(V_n' + V_n),$$
$$Z_n'' - Z_n' = -ic_{44}\,\mu(V_n' + V_n),$$

$$X_n'' + X_n' = -c_{66}(U_n' + U_n) - ic_{66}n(V_n' + V_n),$$
$$Y_n'' + Y_n' = ic_{66}n(U_n' + U_n) - c_{66}(V_n' + V_n),$$

$$X_n'' - X_n' = c_{66}n(U_n' + U_n) + ic_{66}(V_n' + V_n),$$
$$Y_n'' - Y_n' = -ic_{66}(U_n' + U_n) + c_{66}n(V_n' + V_n).$$

We shall show in Section 8 that Eq. (28) under the traction-free boundary conditions at $z = \pm h$ is a Hamiltonian eigensystem. At this point, we carry on solving Eq. (28) by letting

$$\boldsymbol{\psi} = [c_1 \;\; c_2 \;\; c_3 \;\; c_4 \;\; c_5 \;\; c_6]^T e^{\mu z}, \tag{29}$$

then Eq. (28) reduces to

https://doi.org/10.1017/jmech.2014.48 Published online by Cambridge University Press

$$\begin{bmatrix} \lambda & 0 & \hat{c}_{13}\mu & -c_{11}^{-1} & 0 & 0 \\ 0 & \lambda & 0 & 0 & -c_{66}^{-1} & 0 \\ \mu & 0 & \lambda & 0 & 0 & -c_{44}^{-1} \\ 0 & 0 & 0 & \lambda & 0 & \mu \\ 0 & c_{44}\mu^2 & 0 & 0 & \lambda & 0 \\ 0 & 0 & \tilde{c}_{33}\mu^2 & \hat{c}_{13}\mu & 0 & \lambda \end{bmatrix} \begin{bmatrix} c_1 \\ c_2 \\ c_3 \\ c_4 \\ c_5 \\ c_6 \end{bmatrix} = \begin{bmatrix} 0 \\ 0 \\ 0 \\ 0 \\ 0 \\ 0 \end{bmatrix}, \tag{30}$$

which has non-trivial solutions if and only if the determinant of the coefficient matrix equals to zero. This condition yields

$$(c_{44}\kappa^2 + c_{66})\left[c_{33}\,c_{44}\kappa^4 + (c_{11}\,c_{33} - c_{13}^2 - 2c_{13}\,c_{44})\,\kappa^2 + c_{11}\,c_{44}\right] = 0\,,\ (\kappa = \mu/\lambda) \tag{31}$$

which has the roots

$$\kappa_1 = -\kappa_4 = i\left[\frac{c_{11}\,c_{33} - c_{13}(c_{13}+2c_{44}) + \sqrt{(c_{11}\,c_{33} - c_{13}^2)\left[c_{11}c_{33} - (c_{13}+2c_{44})^2\right]}}{2c_{33}\,c_{44}}\right]^{1/2}, \tag{32}$$

$$\kappa_2 = -\kappa_5 = i\left[\frac{c_{11}c_{33} - c_{13}(c_{13}+2c_{44}) - \sqrt{(c_{11}\,c_{33} - c_{13}^2)\left[c_{11}\,c_{33} - (c_{13}+2c_{44})^2\right]}}{2c_{33}\,c_{44}}\right]^{1/2}. \tag{33}$$

$$\kappa_3 = -\kappa_6 = i\sqrt{c_{66}/c_{44}}\,. \tag{34}$$

To each κ_j there corresponds a solution of Eq. (30) determined within a constant. As a result,

$$\begin{bmatrix} U_r \\ U_\theta \\ U_z \\ S_{rr} \\ S_{r\theta} \\ S_{rz} \end{bmatrix}_n = \sum_{j=1}^{3}\left(A_j \begin{bmatrix} f_{1n}(\kappa_j,\,\lambda r) \\ f_{2n}(\kappa_j,\,\lambda r) \\ f_{3n}(\kappa_j,\,\lambda r) \\ f_{4n}(\kappa_j,\,\lambda r) \\ f_{5n}(\kappa_j,\,\lambda r) \\ f_{6n}(\kappa_j,\,\lambda r) \end{bmatrix} e^{\kappa_j \lambda z} + B_j \begin{bmatrix} f_{1n}(-\kappa_j,\,\lambda r) \\ f_{2n}(-\kappa_j,\,\lambda r) \\ f_{3n}(-\kappa_j,\,\lambda r) \\ f_{4n}(-\kappa_j,\,\lambda r) \\ f_{5n}(-\kappa_j,\,\lambda r) \\ f_{6n}(-\kappa_j,\,\lambda r) \end{bmatrix} e^{-\kappa_j \lambda z} \right), \tag{35}$$

$$\begin{bmatrix} S_{\theta\theta} \\ S_{\theta z} \\ S_{zz} \end{bmatrix}_n = \sum_{j=1}^{3}\left(A_j \begin{bmatrix} f_{7n}(\kappa_j,\,\lambda r) \\ f_{8n}(\kappa_j,\,\lambda r) \\ f_{9n}(\kappa_j,\,\lambda r) \end{bmatrix} e^{\kappa_j \lambda z} + B_j \begin{bmatrix} f_{7n}(-\kappa_j,\,\lambda r) \\ f_{8n}(-\kappa_j,\,\lambda r) \\ f_{9n}(-\kappa_j,\,\lambda r) \end{bmatrix} e^{-\kappa_j \lambda z} \right), \tag{36}$$

where A_j and B_j are undetermined constants, and

$$\begin{bmatrix} f_{1n}(\kappa_j,\,\lambda r) \\ f_{2n}(\kappa_j,\,\lambda r) \\ f_{3n}(\kappa_j,\,\lambda r) \\ f_{4n}(\kappa_j,\,\lambda r) \\ f_{5n}(\kappa_j,\,\lambda r) \\ f_{6n}(\kappa_j,\,\lambda r) \end{bmatrix} = \begin{bmatrix} \frac{1}{2}\alpha_j\left[K_{n-1}(\lambda r) + K_{n+1}(\lambda r)\right] \\ i\frac{1}{2}\alpha_j\left[K_{n-1}(\lambda r) - K_{n+1}(\lambda r)\right] \\ (c_{44}\kappa_j^2 + c_{11})K_n(\lambda r) \\ c_{66}\,\alpha_j\left[(n-1)\,K_{n-1}(\lambda r) - (n+1)\,K_{n+1}(\lambda r)\right] + \beta_j\,\kappa_j\,\lambda r K_n(\lambda r) \\ ic_{66}\,\alpha_j\left[(n-1)\,K_{n-1}(\lambda r) + (n+1)\,K_{n+1}(\lambda r)\right] \\ \frac{1}{2}\beta_j\,\lambda r\left[K_{n-1}(\lambda r) + K_{n+1}(\lambda r)\right] \end{bmatrix},$$

$$\begin{bmatrix} f_{7n}(\kappa_j,\,\lambda r) \\ f_{8n}(\kappa_j,\,\lambda r) \\ f_{9n}(\kappa_j,\,\lambda r) \end{bmatrix} = \begin{bmatrix} -c_{66}\,\alpha_j\left[(n-1)\,K_{n-1}(\lambda r) - (n+1)\,K_{n+1}(\lambda r)\right] + \gamma_j\,\lambda r K_n(\lambda r) \\ i\frac{1}{2}\beta_j\lambda r\left[K_{n-1}(\lambda r) - K_{n+1}(\lambda r)\right] \\ \eta_j\,\lambda r K_n(\lambda r) \end{bmatrix},$$

$$\alpha_j = (c_{13} + c_{44})\,\kappa_j,\quad \beta_j = c_{44}(c_{13}\,\kappa_j^2 - c_{11})\,,$$

https://doi.org/10.1017/jmech.2014.48 Published online by Cambridge University Press

$$\gamma_j = \left[c_{44}(c_{13}\kappa_j^2 - c_{12}) + c_{11}\tilde{c}_{23} \right]\kappa_j,$$
$$\eta_j = \left[c_{44}(c_{33}\kappa_j^2 - c_{13}) + c_{11}\tilde{c}_{33} \right]\kappa_j,$$

for $j = 1, 2$, and

$$\begin{bmatrix} f_{1n}(\kappa_3,\ \lambda r) \\ f_{2n}(\kappa_3,\ \lambda r) \\ f_{3n}(\kappa_3,\ \lambda r) \\ f_{4n}(\kappa_3,\ \lambda r) \\ f_{5n}(\kappa_3,\ \lambda r) \\ f_{6n}(\kappa_3,\ \lambda r) \end{bmatrix} = \begin{bmatrix} -i\left[K_{n-1}(\lambda r) - K_{n+1}(\lambda r)\right] \\ K_{n-1}(\lambda r) + K_{n+1}(\lambda r) \\ 0 \\ -2ic_{66}\left[(n-1)K_{n-1}(\lambda r) + (n+1)K_{n+1}(\lambda r)\right] \\ 2c_{66}\left\{\left[(n-1)K_{n-1}(\lambda r) - (n+1)K_{n+1}(\lambda r)\right] - \lambda r K_n(\lambda r)\right\} \\ -ic_{44}\,\kappa_3\lambda r\left[K_{n-1}(\lambda r) - K_{n+1}(\lambda r)\right] \end{bmatrix},$$

$$\begin{bmatrix} f_{7n}(\kappa_3,\ \lambda r) \\ f_{8n}(\kappa_3,\ \lambda r) \\ f_{9n}(\kappa_3,\ \lambda r) \end{bmatrix} = \begin{bmatrix} 2ic_{66}\left[(n-1)K_{n-1}(\lambda r) + (n+1)K_{n+1}(\lambda r)\right] \\ c_{44}\kappa_3\lambda r\left[K_{n-1}(\lambda r) + K_{n+1}(\lambda r)\right] \\ 0 \end{bmatrix}.$$

For isotropy we have $c_{33} = c_{11}$, $c_{13} = c_{12}$, $c_{44} = c_{66} = (c_{11} - c_{12})/2$, Eqs. (32) ~ (33) yield $\kappa_1 = \kappa_2 = i$ and $\kappa_4 = \kappa_5 = -i$, which are repeated. Thus only two eigenvectors are obtained by substituting $\kappa = \pm i$ in Eq. (27). Since a linear combination of the eigenvectors for $\kappa_2 \neq \kappa_1$ is also an eigenvector of a linear system, the other two linearly independent eigenvectors are determined through a limiting process by letting $\kappa_2 \to \kappa_1 = i$ and $\kappa_5 \to \kappa_4 = -i$. A linear combination of these four linearly independent eigenvectors together with the two determined from Eq. (27) produces the solution of Eq. (25) for isotropic materials.

5. EIGENSOLUTION SATISFYING THE TRACTION-FREE BC AT $z = \pm h$

Imposing the traction-free BC: $\sigma_{rz} = \sigma_{\theta z} = \sigma_{zz} = 0$ at $z = \pm h$ on the relevant stress components in Eqs. (35) ~ (36) leads to

$$\begin{bmatrix} \beta_1\lambda_n e^{\kappa_1\lambda_n h} & -\beta_1\lambda_n e^{-\kappa_1\lambda_n h} & \beta_2\lambda_n e^{\kappa_2\lambda_n h} & -\beta_2\lambda_n e^{-\kappa_2\lambda_n h} \\ \beta_1\lambda_n e^{-\kappa_1\lambda_n h} & -\beta_1\lambda_n e^{\kappa_1\lambda_n h} & \beta_2\lambda_n e^{-\kappa_2\lambda_n h} & -\beta_2\lambda_n e^{\kappa_2\lambda_n h} \\ \eta_1\lambda_n e^{\kappa_1\lambda_n h} & \eta_1\lambda_n e^{-\kappa_1\lambda_n h} & \eta_2\lambda_n e^{\kappa_2\lambda_n h} & \eta_2\lambda_n e^{-\kappa_2\lambda_n h} \\ \eta_1\lambda_n e^{-\kappa_1\lambda_n h} & \eta_1\lambda_n e^{\kappa_1\lambda_n h} & \eta_2\lambda_n e^{-\kappa_2\lambda_n h} & \eta_2\lambda_n e^{\kappa_2\lambda_n h} \end{bmatrix} \begin{bmatrix} A_1 \\ B_1 \\ A_2 \\ B_2 \end{bmatrix} = \begin{bmatrix} 0 \\ 0 \\ 0 \\ 0 \end{bmatrix}, \tag{37}$$

$$\begin{bmatrix} \lambda_n e^{\kappa_3\lambda_n h} & -\lambda_n e^{-\kappa_3\lambda_n h} \\ \lambda_n e^{-\kappa_3\lambda_n h} & -\lambda_n e^{\kappa_3\lambda_n h} \end{bmatrix} \begin{bmatrix} A_3 \\ B_3 \end{bmatrix} = \begin{bmatrix} 0 \\ 0 \end{bmatrix}, \tag{38}$$

which have non-trivial solutions if the determinant of the coefficient matrices equal to zero:

$$\begin{vmatrix} \beta_1 e^{\kappa_1\lambda_n h} & -\beta_1 e^{-\kappa_1\lambda_n h} & \beta_2 e^{\kappa_2\lambda_n h} & -\beta_2 e^{-\kappa_2\lambda_n h} \\ \beta_1 e^{-\kappa_1\lambda_n h} & -\beta_1 e^{\kappa_1\lambda_n h} & \beta_2 e^{-\kappa_2\lambda_n h} & -\beta_2 e^{\kappa_2\lambda_n h} \\ \eta_1 e^{\kappa_1\lambda_n h} & \eta_1 e^{-\kappa_1\lambda_n h} & \eta_2 e^{\kappa_2\lambda_n h} & \eta_2 e^{-\kappa_2\lambda_n h} \\ \eta_1 e^{-\kappa_1\lambda_n h} & \eta_1 e^{\kappa_1\lambda_n h} & \eta_2 e^{-\kappa_2\lambda_n h} & \eta_2 e^{\kappa_2\lambda_n h} \end{vmatrix} = 0, \tag{39}$$

$$\begin{vmatrix} e^{\kappa_3\lambda_n h} & -e^{-\kappa_3\lambda_n h} \\ e^{-\kappa_3\lambda_n h} & -e^{\kappa_3\lambda_n h} \end{vmatrix} = 0, \tag{40}$$

where β_1 and β_2 are defined in Eqs. (35) ~ (36), and

$$\eta_j = \left[c_{44}(c_{33}\kappa_j^2 - c_{13}) + 2c_{13}c_{66} \right]\kappa_j.$$

Equations (39) ~ (40) allow us to determine the eigenvalue λ_n, subsequently the associated eigenvectors that satisfy the state equation and the traction-free boundary conditions on the top and bottom surfaces $z = \pm h$. By inspection, Eqs. (39) ~ (40) are satisfied if λ_n is replaced by $-\lambda_n$. So, if λ_n is an eigenvalue, so is $-\lambda_n$. Moreover, $\lambda_0 = 0$ is a common factor of power 4 in Eq. (39) and power 2 in Eq. (40). Thus, $\lambda_0 = 0$ is a repeated eigenvalue. The result is in accord with the symplectic characteristics to be delineated in Section 8, but hardly derivable from a conventional approach.

https://doi.org/10.1017/jmech.2014.48 Published online by Cambridge University Press

6. EIGENSOLUTION FOR $\lambda_0 = 0$

Determination of the linearly independent eigenvectors associated with the repeated eigenvalue $\lambda_0 = 0$ calls for special attention. Knowing that the Bessel function $K_n(\lambda r)$ in (27) approaches $2^{n-1}(n-1)!(\lambda r)^{-n}$ as $\lambda r \to 0$ [15], we attempt to seek the eigensolution for $\lambda_0 = 0$ in the form

$$\boldsymbol{\psi}_0(r, z) = \sum_{k=0}^{\infty} \mathbf{Z}_n^{(k)} r^{\alpha-k}, \quad \mathbf{Z}_n^{(k)} = \left[\mathbf{U}_{nk}(z) \quad r^{-1}\mathbf{S}_{nk}(z) \right]^T, \tag{41}$$

where α is an undetermined parameter, $\mathbf{Z}_n^{(k)}$ are unknown functions of z.

Substituting Eq. (41) in Eq. (25), we obtain

$$\sum_{k=0}^{\infty} \left\{ \mathbf{H}\mathbf{Z}_n^{(k)} + \left[\mathbf{H}_1 - (\alpha - k + 1)\mathbf{I} \right] \mathbf{Z}_n^{(k-1)} + \mathbf{H}_2 \mathbf{Z}_n^{(k-2)} \right\} r^{\alpha-k} = \mathbf{0}, \tag{42}$$

with the traction-free boundary conditions at $z = \pm h$:

$$\sum_{k=0}^{\infty} \left[\mathbf{B}_1 \mathbf{Z}_n^{(k)} + \mathbf{B}_0 \mathbf{Z}_n^{(k-1)} \right]_{z=\pm h} r^{\alpha-k} = \mathbf{0}, \tag{43}$$

where $\mathbf{Z}_n^{(-2)} = \mathbf{Z}_n^{(-1)} = \mathbf{0}$, and

$$\mathbf{H}_1 = \begin{bmatrix} -\hat{c}_{12} & -in\hat{c}_{12} & 0 & 0 & 0 & 0 \\ -in & 1 & 0 & 0 & 0 & 0 \\ 0 & 0 & 0 & 0 & 0 & 0 \\ 0 & 0 & \tilde{c}_{23} d_z & \hat{c}_{12} - 1 & -in & 0 \\ 0 & 0 & -in(\tilde{c}_{23} + c_{44}) d_z & -in\hat{c}_{12} & -2 & 0 \\ -\tilde{c}_{23} d_z & -in(\tilde{c}_{23} + c_{44}) d_z & 0 & 0 & 0 & -1 \end{bmatrix},$$

$$\mathbf{H}_2 = \begin{bmatrix} 0 & 0 & 0 & 0 & 0 & 0 \\ 0 & 0 & 0 & 0 & 0 & 0 \\ 0 & 0 & 0 & 0 & 0 & 0 \\ \tilde{c}_{22} & in\tilde{c}_{22} & 0 & 0 & 0 & 0 \\ -in\tilde{c}_{22} & \tilde{c}_{22} n^2 & 0 & 0 & 0 & 0 \\ 0 & 0 & c_{44} n^2 & 0 & 0 & 0 \end{bmatrix},$$

$$\mathbf{B}_1 = \begin{bmatrix} 0 & 0 & 0 & 0 & 0 & 1 \\ 0 & c_{44}\partial_z & 0 & 0 & 0 & 0 \\ 0 & 0 & \tilde{c}_{33}\partial_z & \hat{c}_{13} & 0 & 0 \end{bmatrix},$$

$$\mathbf{B}_0 = \begin{bmatrix} 0 & 0 & 0 & 0 & 0 & 0 \\ 0 & 0 & inc_{44} & 0 & 0 & 0 \\ \tilde{c}_{23} & in\tilde{c}_{23} & 0 & 0 & 0 & 0 \end{bmatrix}$$

There follow

$$\mathbf{H}\mathbf{Z}_n^{(0)} = \mathbf{0}, \quad \left[\mathbf{B}_1 \mathbf{Z}_n^{(0)} \right]_{z=\pm h} = \mathbf{0}, \tag{44}$$

$$\mathbf{H}\mathbf{Z}_n^{(1)} = -(\mathbf{H}_1 - \alpha\mathbf{I})\mathbf{Z}_n^{(0)}, \quad [\mathbf{B}_1 \mathbf{Z}_n^{(1)} + \mathbf{B}_0 \mathbf{Z}_n^{(0)}]_{z=\pm h} = \mathbf{0}, \tag{45}$$

$$\begin{aligned} &\mathbf{H}\mathbf{Z}_n^{(k)} = -\left[\mathbf{H}_1 - (\alpha - k + 1)\mathbf{I} \right] \mathbf{Z}_n^{(k-1)} - \mathbf{H}_2 \mathbf{Z}_n^{(k-2)}, \\ &[\mathbf{B}_1 \mathbf{Z}_n^{(k)} + \mathbf{B}_0 \mathbf{Z}_n^{(k-1)}]_{z=\pm h} = \mathbf{0}, \quad k \geq 2. \end{aligned} \tag{46}$$

Solving Eqs. (44) ~ (46) successively and substituting the results in (41) yields the eigensolution for $\lambda_0 = 0$. Under the special case of $c_{44} = c_{66}$, it turns out that $\mathbf{Z}_n^{(k)} = 0$ for $k \geq 3$ and the six linearly independent eigenvectors are

$$\boldsymbol{\psi}_{01}^{(0)} = \begin{bmatrix} 1 \\ 0 \\ 0 \\ 0 \\ 0 \\ 0 \end{bmatrix} r^{-1} + \begin{bmatrix} 0 \\ 0 \\ 0 \\ -2c_{66} \\ 0 \\ 0 \end{bmatrix} r^{-2}, \quad \boldsymbol{\psi}_{02}^{(0)} = \begin{bmatrix} 0 \\ 1 \\ 0 \\ 0 \\ 0 \\ 0 \end{bmatrix} r^{-1} + \begin{bmatrix} 0 \\ 0 \\ 0 \\ 0 \\ -2c_{66} \\ 0 \end{bmatrix} r^{-2}, \tag{47}$$

$$\boldsymbol{\psi}_{03}^{(0)} = \begin{bmatrix} 0 \\ 0 \\ 1 \\ 0 \\ 0 \\ 0 \end{bmatrix}, \quad \boldsymbol{\psi}_{05}^{(0)} = \begin{bmatrix} 1 \\ 0 \\ 0 \\ 0 \\ 0 \\ 0 \end{bmatrix} r + \begin{bmatrix} 0 \\ 0 \\ -2c_{33}^{-1} c_{13} z \\ c_{33}^{-1} c_{13} \gamma_2 / \gamma_1 \\ 0 \\ 0 \end{bmatrix}, \quad \boldsymbol{\psi}_{06}^{(0)} = \begin{bmatrix} 0 \\ 1 \\ 0 \\ 0 \\ 0 \\ 0 \end{bmatrix} r, \tag{48}$$

for $n = 0$, and

$$\boldsymbol{\psi}_{01}^{(n)} = \begin{bmatrix} 1 \\ i \\ 0 \\ 0 \\ 0 \\ 0 \end{bmatrix} r^{n-1} + \begin{bmatrix} 0 \\ 0 \\ 0 \\ 2c_{66}(n-1) \\ 2ic_{66}(n-1) \\ 0 \end{bmatrix} r^{n-2},$$

$$\boldsymbol{\psi}_{02}^{(n)} = \begin{bmatrix} 1 \\ -i \\ 0 \\ 0 \\ 0 \\ 0 \end{bmatrix} r^{-n-1} + \begin{bmatrix} 0 \\ 0 \\ 0 \\ -2c_{66}(n+1) \\ 2ic_{66}(n+1) \\ 0 \end{bmatrix} r^{-n-2}, \tag{49}$$

$$\boldsymbol{\psi}_{03}^{(n)} = \begin{bmatrix} 0 \\ 0 \\ -1 \\ 0 \\ 0 \\ 0 \end{bmatrix} n^{-1} r^{n} + \begin{bmatrix} z \\ iz \\ 0 \\ 0 \\ 0 \\ 0 \end{bmatrix} r^{n-1} + \begin{bmatrix} 0 \\ 0 \\ 0 \\ 2c_{66}(n-1)z \\ 2ic_{66}(n-1)z \\ 0 \end{bmatrix} r^{n-2}, \tag{50}$$

$$\boldsymbol{\psi}_{04}^{(n)} = \begin{bmatrix} 0 \\ 0 \\ 1 \\ 0 \\ 0 \\ 0 \end{bmatrix} n^{-1} r^{-n} + \begin{bmatrix} z \\ -iz \\ 0 \\ 0 \\ 0 \\ 0 \end{bmatrix} r^{-n-1} + \begin{bmatrix} 0 \\ 0 \\ 0 \\ -2c_{66}(n+1)z \\ 2ic_{66}(n+1)z \\ 0 \end{bmatrix} r^{-n-2}, \tag{51}$$

https://doi.org/10.1017/jmech.2014.48 Published online by Cambridge University Press

$$\boldsymbol{\psi}_{05}^{(n)} = \begin{bmatrix} \chi_{n1} \\ i\chi_{n2} \\ 0 \\ 0 \\ 0 \\ 0 \end{bmatrix} n^{-1} r^{n+1} + \begin{bmatrix} 0 \\ 0 \\ -z \\ -\chi_{n3} \\ -i\chi_{n4} \\ 0 \end{bmatrix} n^{-1} r^{n} + \begin{bmatrix} z^2/2 \\ iz^2/2 \\ 0 \\ 0 \\ 0 \\ 0 \end{bmatrix} r^{n-1} + \begin{bmatrix} 0 \\ 0 \\ 0 \\ c_{66}(n-1)z^2 \\ ic_{66}(n-1)z^2 \\ 0 \end{bmatrix} r^{n-2}, \tag{52}$$

$$\boldsymbol{\psi}_{06}^{(n)} = \begin{bmatrix} \chi_{-n1} \\ -i\chi_{-n2} \\ 0 \\ 0 \\ 0 \\ 0 \end{bmatrix} n^{-1} r^{-n+1} + \begin{bmatrix} 0 \\ 0 \\ z \\ \chi_{-n3} \\ i\chi_{-n4} \\ 0 \end{bmatrix} n^{-1} r^{-n} + \begin{bmatrix} z^2/2 \\ -iz^2/2 \\ 0 \\ 0 \\ 0 \\ 0 \end{bmatrix} r^{-n-1} + \begin{bmatrix} 0 \\ 0 \\ 0 \\ -c_{66}(n+1)z^2 \\ ic_{66}(n+1)z^2 \\ 0 \end{bmatrix} r^{-n-2}, \tag{53}$$

for $n \geq 1$, where

$$\begin{bmatrix} \chi_{n1} \\ \chi_{n2} \\ \chi_{n3} \\ \chi_{n4} \end{bmatrix} = \begin{bmatrix} \left(\dfrac{4c_{33}c_{66}}{c_{11}+c_{12}} - n\gamma_2 \right) / \left[8\gamma_1 (n+1) c_{66} \right] \\ \left(-\dfrac{4c_{33}(c_{11} - c_{33}^{-1}c_{13}^2)}{c_{11}+c_{12}} - n\gamma_2 \right) / \left[8\gamma_1 (n+1) c_{66} \right] \\ (n-2)\gamma_2 / (4\gamma_1) \\ n\gamma_2 / (4\gamma_1) \end{bmatrix},$$

$$\begin{bmatrix} \chi_{-n1} \\ \chi_{-n2} \\ \chi_{-n3} \\ \chi_{-n4} \end{bmatrix} = \begin{bmatrix} \left(\dfrac{4c_{33}c_{66}}{c_{11}+c_{12}} + n\gamma_2 \right) / \left[8\gamma_1 (n-1) c_{66} \right] \\ \left(-\dfrac{4c_{33}(c_{11} - c_{33}^{-1}c_{13}^2)}{c_{11}+c_{12}} + n\gamma_2 \right) / \left[8\gamma_1 (n-1) c_{66} \right] \\ -(n+2)\gamma_2 / (4\gamma_1) \\ n\gamma_2 / (4\gamma_1) \end{bmatrix},$$

$$\gamma_1 = \frac{c_{13}}{c_{11}+c_{12}}, \quad \gamma_2 = \frac{c_{33}(c_{11}+c_{12}) - 2c_{13}^2}{c_{11}+c_{12}}.$$

A combination of all the linearly independent eigenvectors yields the complete solution of the state equation, which satisfies the traction-free boundary conditions at $z = \pm h$:

$$[u_r \ u_\theta \ u_z \ \sigma_{rr} \ \sigma_{r\theta} \ \sigma_{rz}]^T = \sum_{n=-\infty}^{\infty} \mathbf{F}_n(r,z) e^{in\theta}, \tag{54}$$

where

$$\mathbf{F}_n(r,z) = A_{n0}\boldsymbol{\psi}_{01}^{(n)} + A'_{n0}\boldsymbol{\psi}_{05}^{(n)} + B_{n0}\boldsymbol{\psi}_{02}^{(n)} + B'_{n0}\boldsymbol{\psi}_{06}^{(n)} + \sum_{k=1}^{\infty} A_{nk}\mathbf{X}_{nk},$$

$$\mathbf{X}_{nk} = \mathbf{K}_n(\lambda_k r)\boldsymbol{\psi}_k^{(n)}(z) + \mathbf{R}_n(\lambda_k r, z),$$

in which we have dropped the eigenvectors $\boldsymbol{\psi}_{03}^{(n)}$ and $\boldsymbol{\psi}_{04}^{(n)}$ in which $(S_{rr})_n$ and $(S_{r\theta})_n$ are anti-symmetric to z and dropped those eigenvectors corresponding to κ_3 which lead to $(U_z)_n = 0$ and $(S_{zz})_n = 0$. The explicit expressions of the eigenvector $\boldsymbol{\psi}_k^{(n)}$ and the matrices $\mathbf{K}_n$, $\mathbf{R}_n$ are given in the appendix A.

7. SATISFACTION OF THE BC AT $r = a$ AND $r \to \infty$

Imposing the loading conditions (7) at $r \to \infty$ on Eq. (54), we obtain

$$\mathbf{F}_0(\infty, z) = A_{00}\left[\boldsymbol{\psi}_{01}^{(0)}\right]_{r\to\infty} + A'_{00}\left[\boldsymbol{\psi}_{05}^{(0)}\right]_{r\to\infty} + B_{00}\left[\boldsymbol{\psi}_{02}^{(0)}\right]_{r\to\infty} + B'_{00}\left[\boldsymbol{\psi}_{06}^{(0)}\right]_{r\to\infty}, \tag{55}$$

$$\mathbf{F}_2(\infty, z) = A_{20}\left[\boldsymbol{\psi}_{01}^{(2)}\right]_{r\to\infty} + A'_{20}\left[\boldsymbol{\psi}_{05}^{(2)}\right]_{r\to\infty} + B_{20}\left[\boldsymbol{\psi}_{02}^{(2)}\right]_{r\to\infty} + B'_{20}\left[\boldsymbol{\psi}_{06}^{(2)}\right]_{r\to\infty}, \tag{56}$$

where the series terms in Eq. (54) vanish for $K_n(\lambda_k r)|_{r\to\infty} \to 0$; $\mathbf{F}_0(\infty, z)$ and $\mathbf{F}_2(\infty, z)$ contain the unknown displacements at $r \to \infty$ such that

$$\mathbf{F}_0(\infty, z) = \begin{bmatrix} U_0(\infty, z) \\ V_0(\infty, z) \\ W_0(\infty, z) \\ p/2 \\ 0 \\ 0 \end{bmatrix}, \quad \mathbf{F}_2(\infty, z) = \begin{bmatrix} U_2(\infty, z) \\ V_2(\infty, z) \\ W_2(\infty, z) \\ p/2 \\ -p/2 \\ 0 \end{bmatrix}.$$

Imposing the traction-free boundary conditions (8) at $r = a$ on Eq. (54), we obtain

$$\mathbf{F}_0(a, z) = A_{00}\left[\boldsymbol{\psi}_{01}^{(0)}\right]_{r=a} + A'_{00}\left[\boldsymbol{\psi}_{05}^{(0)}\right]_{r=a} + B_{00}\left[\boldsymbol{\psi}_{02}^{(0)}\right]_{r=a} + B'_{00}\left[\boldsymbol{\psi}_{06}^{(0)}\right]_{r=a} + \sum_{k=1}^{\infty} A_{0k}(\mathbf{X}_{0k})_{r=a}, \tag{57}$$

$$\mathbf{F}_2(a, z) = A_{20}\left[\boldsymbol{\psi}_{01}^{(2)}\right]_{r=a} + A'_{20}\left[\boldsymbol{\psi}_{05}^{(2)}\right]_{r=a} + B_{20}\left[\boldsymbol{\psi}_{02}^{(2)}\right]_{r=a} + B'_{20}\left[\boldsymbol{\psi}_{06}^{(2)}\right]_{r=a} + \sum_{k=1}^{\infty} A_{2k}(\mathbf{X}_{2k})_{r=a}, \tag{58}$$

where $\mathbf{F}_0(a, z)$ and $\mathbf{F}_2(a, z)$ contain the unknown displacements at $r = a$ such that

https://doi.org/10.1017/jmech.2014.48 Published online by Cambridge University Press

$$\mathbf{F}_0(a,\,z)=\begin{bmatrix}U_0(a,\,z)\\ V_0(a,\,z)\\ W_0(a,\,z)\\ 0\\ 0\\ 0\end{bmatrix},\quad \mathbf{F}_2(a,\,z)=\begin{bmatrix}U_2(a,\,z)\\ V_2(a,\,z)\\ W_2(a,\,z)\\ 0\\ 0\\ 0\end{bmatrix}.$$

By comparing the coefficients on both sides of Eqs. (55) ~ (58), there follows

$$A_{00}=\frac{pa^2}{4c_{66}},\quad B_{00}=A_{0k}=0,\quad A'_{00}=\frac{p}{2}\left(c_{13}^{-1}c_{33}\frac{\beta_1}{\beta_2}\right),$$
$$A_{20}=\frac{p}{4c_{66}},\quad A'_{20}=0, \tag{59}$$

$$B_{20}\left[\boldsymbol{\psi}_{02}^{(2)}\right]_{r=a}+B'_{20}\left[\boldsymbol{\psi}_{06}^{(2)}\right]_{r=a}+\sum_{k=1}^{\infty}A_{2k}(\mathbf{X}_{2k})_{r=a}$$
$$=\mathbf{F}_2(a,\,z)-\frac{p}{4c_{66}}\left[\boldsymbol{\psi}_{01}^{(2)}\right]_{r=a}, \tag{60}$$

where the constants B_{20}, B'_{20} and A_{2k} (k = 1, 2, ⋯) in Eq. (60) are to be determined. In what follows, we delineate the Hamiltonian characteristics and symplectic orthogonality of the eigensystem associated with Eq. (28), which are indispensable for using eigenfunction expansion to determine the unknown constants.

8. SYMPLECTIC CHARACTERISTICS

To facilitate exposition, let us express the eigensystem given by Eq. (28) under the traction-free boundary conditions at $z = \pm h$ as

$$\mathbf{H}\boldsymbol{\psi}=\lambda\boldsymbol{\psi},\quad \mathbf{B}(\boldsymbol{\psi})=\mathbf{0}, \tag{61}$$

where λ is the eigenvalue, $\boldsymbol{\psi}$ is the associated eigenvector. The system matrix $\mathbf{H}$ exhibits the feature such that the matrix operators $\mathbf{L}_{11}$, $\mathbf{L}_{11}^*$ are adjoint and $\mathbf{L}_{12}$, $\mathbf{L}_{21}$ are symmetric. Such a feature is essential for the symplectic characteristics delineated as follows.

First of all, the adjoint system of Eq. (61) is

$$\mathbf{H}\boldsymbol{\varphi}=-\lambda\boldsymbol{\varphi},\quad \mathbf{B}(\boldsymbol{\varphi})=\mathbf{0}, \tag{62}$$

where the star $*$ denotes the adjoint, $\boldsymbol{\phi}$ is the eigenvector associated with the eigenvalue −λ, and

$$\boldsymbol{\varphi}=\begin{bmatrix}\tilde{\mathbf{U}}_n\\ \tilde{\mathbf{S}}_n\end{bmatrix},\quad \tilde{\mathbf{U}}_n=\begin{bmatrix}\tilde{U}_n\\ \tilde{V}_n\\ \tilde{W}_n\end{bmatrix},\quad \tilde{\mathbf{S}}_n=\begin{bmatrix}\tilde{X}_n\\ \tilde{Y}_n\\ \tilde{Z}_n\end{bmatrix}.$$

Derivation begins with the equality

$$\int_{-h}^{h}\boldsymbol{\varphi}^T\mathbf{J}\mathbf{H}\boldsymbol{\psi}\,dz$$
$$=\int_{-h}^{h}\left[\tilde{\mathbf{U}}_n^T(\mathbf{L}_{21}\mathbf{U}_n-\mathbf{L}_{11}^*\mathbf{S}_n)-\tilde{\mathbf{S}}_n^T(\mathbf{L}_{11}\mathbf{U}_n+\mathbf{L}_{12}\mathbf{S}_n)\right]dz, \tag{63}$$

where $\mathbf{J}=\begin{bmatrix}\mathbf{0} & \mathbf{I}\\ -\mathbf{I} & \mathbf{0}\end{bmatrix}_{6\times6}$, $\mathbf{I}$ is the 3 × 3 identity matrix.

Applying Green's theorem to the right-hand side of (63) yields

$$\int_{-h}^{h}\boldsymbol{\varphi}^T\mathbf{J}\mathbf{H}\boldsymbol{\psi}\,dz$$
$$=\int_{-h}^{h}\left[\tilde{\mathbf{U}}_n^T(\mathbf{L}_{21}\mathbf{U}_n-\mathbf{L}_{11}^*\mathbf{S}_n)-\tilde{\mathbf{S}}_n^T(\mathbf{L}_{11}\mathbf{U}_n+\mathbf{L}_{12}\mathbf{S}_n)\right]dz+\mathbf{B}(\boldsymbol{\varphi})$$
$$=\int_{-h}^{h}\boldsymbol{\psi}^T\mathbf{J}\mathbf{H}\boldsymbol{\varphi}\,dz+\mathbf{B}(\boldsymbol{\varphi}), \tag{64}$$

in which $B(\boldsymbol{\phi})$ denotes the boundary integral term. This shows that $\mathbf{JH}$ is self-adjoint such that $(\mathbf{JH})^* = \mathbf{JH}$.

Next, pre-multiplying Eq. (61) by $\boldsymbol{\phi}^T\mathbf{J}$, integrating it through the thickness and taking transpose, with $\mathbf{J}^T = -\mathbf{J}$, we obtain

$$\int_{-h}^{h}\boldsymbol{\varphi}^T\mathbf{J}\mathbf{H}\boldsymbol{\psi}\,dz=\lambda\int_{-h}^{h}\boldsymbol{\varphi}^T\mathbf{J}\boldsymbol{\psi}\,dz=-\lambda\int_{-h}^{h}\boldsymbol{\psi}^T\mathbf{J}\boldsymbol{\varphi}\,dz, \tag{65}$$

which, upon substituting into (64), becomes

$$\int_{-h}^{h}\boldsymbol{\psi}^T\mathbf{J}(\mathbf{H}\boldsymbol{\varphi}+\lambda\boldsymbol{\varphi})\,dz+B(\boldsymbol{\varphi})=0. \tag{66}$$

There follows the adjoint system given by () which reveals that if λ is an eigenvalue, so is −λ. This property is confirmed by the results obtained earlier. Since the eigenvalues appear in (λ, −λ) pairs, to bring out the symplectic orthogonality of the eigenvectors, it is necessary to arrange them as follows:

(1) the eigenvectors $\boldsymbol{\psi}_k^{(n)}$ (k = 1, 2, ⋯) associated with the eigenvalues λ_k.

(2) the eigenvectors $\boldsymbol{\psi}_{-k}^{(n)}\equiv\boldsymbol{\varphi}$ (i = 1, 2; k = 1, 2, ⋯) associated with the eigenvalues λ_{-k} (= λ_{-k}).

(3) the eigenvectors $\boldsymbol{\psi}_0^{(n)}$ associated with the repeated eigenvalue $\lambda_0 = 0$.

Having shown that the eigensystem is a Hamiltonian system, following the same line as in [13,16], we can derive the symplectic orthogonality of the eigenvectors:

$$\int_{-h}^{h}\left[\boldsymbol{\psi}_p^{(n)}\right]^T\mathbf{J}\boldsymbol{\psi}_q^{(n)}\,dz\begin{cases}=0 & \text{for } q\neq -p\\ \neq 0 & \text{for } q=-p\end{cases} \tag{67}$$

for the eigenvectors associated with non-zero eigenvalues, and

$$\int_{-h}^{h}\left[\boldsymbol{\psi}_{0\alpha}^{(n)}\right]^T\mathbf{J}\boldsymbol{\psi}_{0\beta}^{(n)}dz\begin{cases}=0, & |\beta-\alpha|\neq 4\\ \neq 0, & |\beta-\alpha|=4\end{cases}$$
$$(\alpha,\,\beta=1,\,3,\,5 \text{ or } 2,\,4,\,6) \tag{68}$$

for the eigenvectors associated with the repeated eigenvalue $\lambda_0 = 0$.

https://doi.org/10.1017/jmech.2014.48 Published online by Cambridge University Press

9. SYMPLECTIC EIGENFUNCTION EXPANSION

Having derived the symplectic orthogonality of the eigenvectors, we are in a position to determine the unknown constants in (60) by means of eigenfunction expansion in the state space. To this end, multiplying (60) by $\left[\boldsymbol{\psi}_{0k}^{(n)}\right]_{r=a}^{T}\mathbf{J}$ (k = 2, 6) and $(\mathbf{X}_{2k})_{r=a}^{T}\mathbf{J}$ (k = 1, 2, ⋯) respectively and integrating the resulting equations, with the orthogonality relations (67) and (68) we obtain

$$\int_{-h}^{h}\left[\boldsymbol{\psi}_{02}^{(2)}\right]_{r=a}^{T}\mathbf{J}\left\{\mathbf{F}_2(a,\,z)-\frac{p}{4c_{66}}\left[\boldsymbol{\psi}_{01}^{(2)}\right]_{r=a}\right\}dz$$
$$=B_{20}'\int_{-h}^{h}\left[\boldsymbol{\psi}_{02}^{(2)}\right]_{r=a}^{T}\mathbf{J}\left[\boldsymbol{\psi}_{06}^{(2)}\right]_{r=a}dz, \tag{69}$$

$$\int_{-h}^{h}\left[\boldsymbol{\psi}_{06}^{(2)}\right]_{r=a}^{T}\mathbf{J}\left\{\mathbf{F}_2(a,z)-\frac{p}{4c_{66}}\left[\boldsymbol{\psi}_{01}^{(2)}\right]_{r=a}\right\}dz$$
$$=B_{20}\int_{-h}^{h}\left[\boldsymbol{\psi}_{06}^{(2)}\right]_{r=a}^{T}\mathbf{J}\left[\boldsymbol{\psi}_{02}^{(2)}\right]_{r=a}dz, \tag{70}$$

$$\int_{-h}^{h}(\mathbf{X}_{2k})_{r=a}^{T}\mathbf{J}\left\{\mathbf{F}_2(a,\,z)-\frac{p}{4c_{66}}\left[\boldsymbol{\psi}_{01}^{(2)}\right]_{r=a}\right\}dz=0, \tag{71}$$

where the expression $(\mathbf{X}_{2p})_{r=a}^{T}\mathbf{J}(\mathbf{X}_{2q})_{r=a}$ can be reduced to expression containing $\boldsymbol{\psi}_p^{T}\mathbf{J}\boldsymbol{\psi}_q$ and then the symplectic orthogonality is applicable, as derived in the appendix B.

Equations (69) ~ (71) constitute a system of integral equations, and the unknowns $U_2(a, z)$, $V_2(a, z)$ and $W_2(a, z)$ in $\mathbf{F}_2(a, z)$ are related to the constants B_{20}, B_{20}' and A_{2k} by Eq. (58). Thus, substituting the relevant component equations of Eq. (58) in Eqs. (69) ~ (71), taking N terms of the series for computation, we arrive at a system of $N + 2$ algebraic equations (2 equations from Eq. (69) ~ (70); N equations from Eq. (71) for (k = 1, 2, … N) for the $N + 2$ unknowns (B_{20}, B_{20}' and A_{2k}, k = 1, 2, … N), which can be easily solved by using a standard method for simultaneous linear algebraic equations.

10. RESULTS AND DISCUSSIONS

To examine quantitatively the stress concentration factor, the following non-dimensional values of the elastic constants are taken for computation: c_{33} / c_{11} = 1 (isotropic material), 5, 10, 20 and c_{12} / c_{11} = c_{13} / c_{11} = c_{44} / c_{11} = 1/3 for transversely isotropic materials. These values are typical for engineering materials, ranging from aluminum to epoxy-based fiber-reinforced composites such as glass/epoxy and graphite/epoxy. The dimensions of the plate are taken to be a/h = 1 ~ 8.

In evaluating the displacements and stresses in the plate, for the convergence, in principle the number N can be chosen as large as necessary to achieve a required accuracy. For the material constants used in computations, taking less than 20 terms of the series produces convergent results at locations away from the circular hole boundary $r = a$. Convergence of the stresses at the boundary is relatively slow and the results are oscillating due to geometric discontinuity, it is necessary to take up to 40 terms to achieve satisfactory convergence. Figure 2 shows the results by taking 20, 30, and 40 terms of the series for computation. Displacements and stresses in region away from the boundary converge rapidly (requiring less than 20 terms), but in region where the end effect is significant convergence is relatively slow (requiring up to 40 terms).

Figures 3 and 4 show the variations of the stress concentration factor for different transverse isotropy and different plate radius to thickness ratios, a/h, at middle planes and surfaces, respectively. Since our approach using eigenfunction expansion can only determine the 3D solutions of plates whose characteristic size a is greater than (or equal to) the thickness h, as a result this work is limited to the cases where $a/h \geq 1$. With decreasing a/h, the stress concentration factor increases at middle planes and decreases at surfaces. Their minimum values are less than and maximum values are more than that provided by the 2D solution, where it's equal to 3. The stronger anisotropy, c_{33} / c_{11}, means the stronger resistance and more uniform stress distributions in the thickness direction. For weaker anisotropy, the stress concentration factor is farer away from the 2D solution. A comparison of $(\sigma_{\theta\theta}/p)_{\max}$ / $(\sigma_{\theta\theta}/p)_{2D}$ = 1.08 on middle plane for the ratio of a/h = 1 of isotropic material with 1.05 of the finite element solution by Li *et al*. [4] shows a very good agreement. Moreover, the difference of $(\sigma_{\theta\theta}/p)_{\min}$ / $(\sigma_{\theta\theta}/p)_{\max}$ is minimal as can be seen by the comparison of our result, 0.82, with that of Li *et al*., 0.84.

Figure 5 depicts the stress concentration factor contour, $\sigma_{\theta\theta}/p$, on middle plane of isotropic plate under remote extension. The strongest tension stress and compression stress happen at the boundary $r = a$ with $\theta = \pm\pi/2$ and $\theta = 0$, π, respectively. Then the stresses decay away from the boundary. The stress concentration factor contours on surfaces, $z = \pm h$, have great resemblances to that of Fig. 5, except the magnitude everywhere due to non-uniform distributions along the thickness.

The results shown in Fig. 6 are the variations of the stress concentration factor, $\sigma_{\theta\theta}/p$, at $r = a$ and $\theta = \pi/2$ for various a/h and for transversely isotropic and isotropic materials. They show the stress concentration factor is sensitive to the ratio a/h and to transversely isotropy. The stress concentration factor attains its maximum in the middle of the plate and decreases as approaching the free surfaces. As the ratio a/h decreases further or as the transversely isotropy is weaker, the magnitudes of the maximum increase and the magnitudes of the minimum decreases. The 2D solutions are not reliable in both situations.

Figures 7 and 8 show the variations of the stress concentration factor, $\sigma_{\theta\theta}/p$, and stress ratio σ_{rr} / $\sigma_{\theta\theta}$ of

https://doi.org/10.1017/jmech.2014.48 Published online by Cambridge University Press

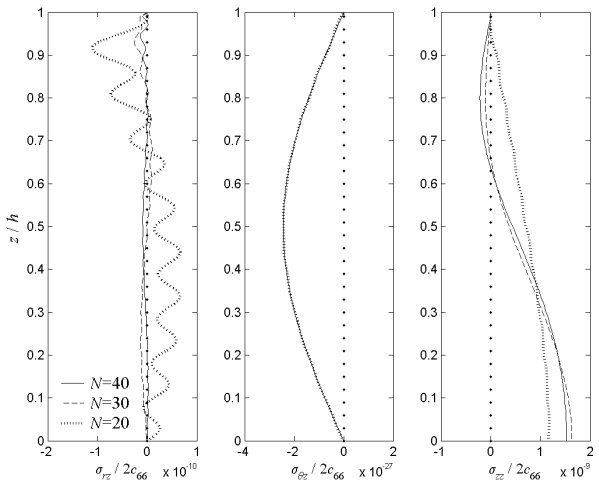


Fig. 2 Convergence of the stresses at the rim by taking 20, 30, and 40 terms of the series for computation.

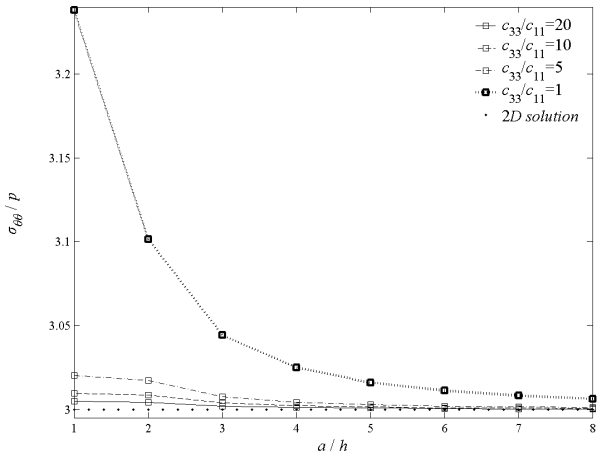


Fig. 3 Stress concentration factors due to different *a*/*h* ratios at the middle planes of transversely isotropic plates.

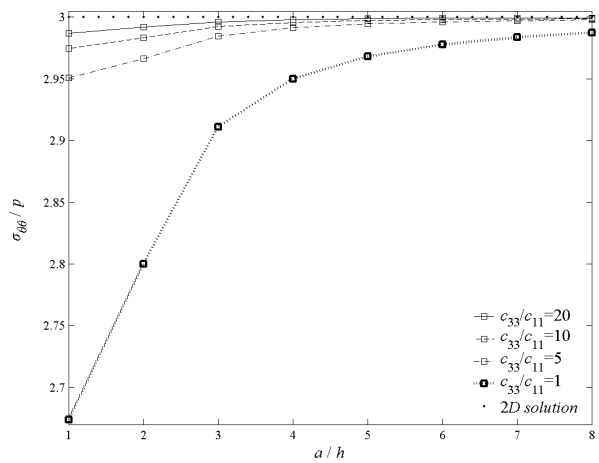


Fig. 4 Stress concentration factors due to different *a*/*h* ratios at the surfaces of transversely isotropic plates.

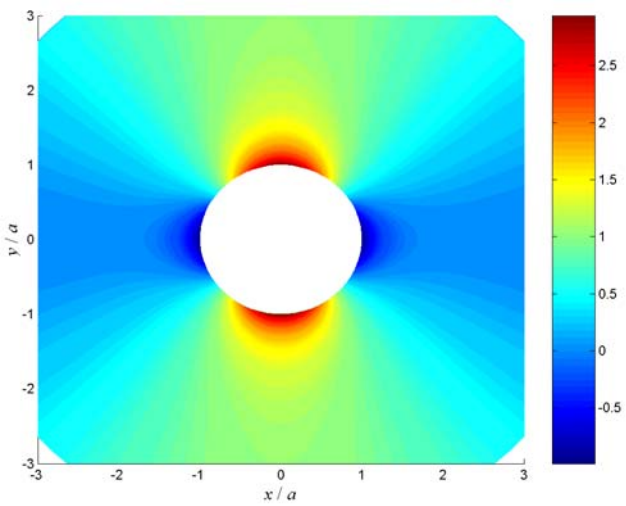


Fig. 5 Stress contours at the middle plane of an isotropic plate.

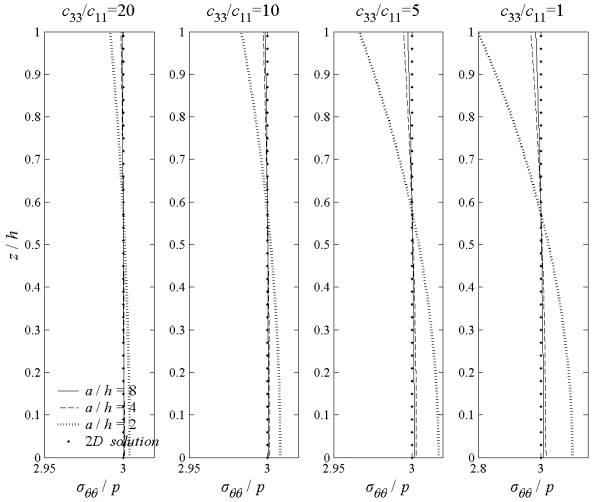


Fig. 6 Variations of the Stress concentration factors of different c_{33} / c_{11} through the thickness.

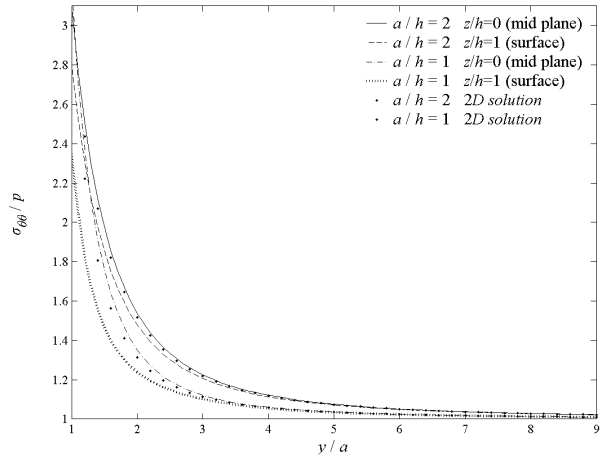


Fig. 7 Variation of the Stress concentration factor normal to the direction of the extension.

https://doi.org/10.1017/jmech.2014.48 Published online by Cambridge University Press

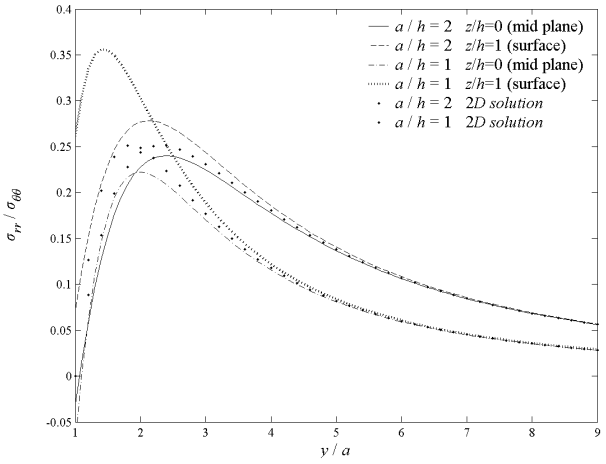


Fig. 8 Variation of the radial Stress at θ = π/2 along *y* axis.

isotropic material in front of notch root on different plane layer for *a*/*h* = 2 and *a*/*h* = 1. The curves are different to 2D solutions on different plane layer and are sensitive to the location of plane layer and the ratio *a*/*h*. The 2D solutions can describe the distributions well away from the notch, near mid plane or with larger *a*/*h*, but differ significantly from 3D results in the vicinity of the hole, in region near the plane surface or with smaller *a*/*h*. As *y* increases, the stresses approach to the 2D solutions rapidly. A comparison of $(\sigma_{\theta\theta} / p) / (\sigma_{\theta\theta} / p)_{\max}$ at $y = 4h$, where decay turns slow, our result, 0.35, is identical to that obtained by Li *et al*. The peak, (location, value) = (1.8, 0.23), of $\sigma_{rr} / \sigma_{\theta\theta}$ on middle plane along *y* / *a* with that, (1.6, 0.25), of Li *et al*. shows the agreement is good.

11. CONCLUSIONS

A Hamiltonian state-space approach for 3D exact analysis of an elastic plate, of transversely isotropic elastic materials, containing a circular hole under remote loading has been developed. We have delineated the Hamiltonian characteristics and symplectic orthogonality of the eigensystem inherent in the formulation, thus we can seek the 3D solution by using separation of variables and eigenfunction expansion in the symplectic state space. The study shows that, when the transversely isotropic plate is subjected to remote loading, the stress concentration factor are sensitive to the ratio *a*/*h* and to transversely isotropy, and the radius stress of isotropic material in front of notch root on different plane layer are sensitive to the location of plane layer and the ratio *a*/*h*. As the ratio *a*/*h* increases further, the transversely isotropy is stronger, or the location is farer away from the notch or near mid plane, the 2D solutions are applicable.

ACKNOWLEDGMENTS

The work is supported by the National Science Council of Taiwan, ROC through grants NSC99-2221-E006-067-MY3.

APPENDIX

A. EXPRESSIONS OF MATRICES AND VECTORS IN EQUATION (54)

Expressions of matrices and vectors in Eq. (54) are

$$\boldsymbol{\psi}_k(z) = \begin{bmatrix} \psi_{1k}(z) \\ \psi_{2k}(z) \\ \psi_{3k}(z) \\ \psi_{4k}(z) \\ \psi_{5k}(z) \\ \psi_{6k}(z) \end{bmatrix} = \begin{bmatrix} \sum_{j=1}^{2} \alpha_j \left[(A_{jk} / A_k) e^{\kappa_j \lambda_{1k} z} + (B_{jk} / A_k) e^{-\kappa_j \lambda_{1k} z} \right] \\ 0 \\ \sum_{j=1}^{2} (c_{44} \kappa_j^2 + c_{11}) \left[(A_{jk} / A_k) e^{\kappa_j \lambda_{1k} z} - (B_{jk} / A_k) e^{-\kappa_j \lambda_{1k} z} \right] \\ \sum_{j=1}^{2} \beta_j \kappa_j \lambda_{1k} \left[(A_{jk} / A_k) e^{\kappa_j \lambda_{1k} z} + (B_{jk} / A_k) e^{-\kappa_j \lambda_{1k} z} \right] \\ 0 \\ \sum_{j=1}^{2} \beta_j \lambda_{1k} \left[(A_{jk} / A_k) e^{\kappa_j \lambda_{1k} z} - (B_{jk} / A_k) e^{-\kappa_j \lambda_{1k} z} \right] \end{bmatrix}, \tag{A1}$$

$$\mathbf{K}_n(\lambda_k r) = \begin{bmatrix} \nu_{1n}(\lambda_k r) & 0 & 0 & 0 & 0 & 0 \\ 0 & 0 & 0 & 0 & 0 & 0 \\ 0 & 0 & K_n(\lambda_k r) & 0 & 0 & 0 \\ 0 & 0 & 0 & K_n(\lambda_k r) & 0 & 0 \\ 0 & 0 & 0 & 0 & 0 & 0 \\ 0 & 0 & 0 & 0 & 0 & \nu_{1n}(\lambda_k r) \end{bmatrix}, \quad \mathbf{R}_n(\lambda_k r,\ z) = \begin{bmatrix} 0 \\ -\upsilon_{1n}(\lambda_k r) \\ 0 \\ \nu_{4n}(\lambda_k r) \\ -\upsilon_{4n}(\lambda_k r) \\ 0 \end{bmatrix} \psi_{1k}(z), \tag{A2}$$

where

$$\nu_{1n}(\lambda_k r) = \frac{1}{2}\left[K_{n-1}(\lambda_k r) + K_{n+1}(\lambda_k r) \right],$$

https://doi.org/10.1017/jmech.2014.48 Published online by Cambridge University Press

$$\upsilon_{1n}(\lambda_k r)=\frac{1}{2}\left[K_{n-1}(\lambda_k r)-K_{n+1}(\lambda_k r)\right],$$

$$\nu_{4n}(\lambda_k r)=c_{66}\left[(n-1)K_{n-1}(\lambda_k r)-(n+1)K_{n+1}(\lambda_k r)\right],$$

$$\upsilon_{4n}(\lambda_k r)=c_{66}\left[(n-1)K_{n-1}(\lambda_k r)+(n+1)K_{n+1}(\lambda_k r)\right].$$

B. SYMPLECTIC ORTHOGONALITY RELATION IN EQUATION (71)

Since

$$\begin{aligned}(\mathbf{X}_{np})_{r=a}^{T}\mathbf{J}(\mathbf{X}_{nq})_{r=a}&=\left[\mathbf{K}_n(\lambda_p a)\boldsymbol{\psi}_p(z)+\mathbf{R}_n(\lambda_p a,\ z)\right]^T\mathbf{J}\left[\mathbf{K}_n(\lambda_q a)\boldsymbol{\psi}_q(z)+\mathbf{R}_n(\lambda_q a,\ z)\right]\\&=\left[\mathbf{K}_n(\lambda_p a)\boldsymbol{\psi}_p(z)\right]^T\mathbf{J}\left[\mathbf{K}_n(\lambda_q a)\boldsymbol{\psi}_q(z)\right]\\&\quad+\left[\mathbf{K}_n(\lambda_p a)\boldsymbol{\psi}_p(z)\right]^T\mathbf{J}\left[\mathbf{R}_n(\lambda_q a,\ z)\right]+\left[\mathbf{R}_n(\lambda_p a,\ z)\right]^T\mathbf{J}\left[\mathbf{K}_n(\lambda_q a)\boldsymbol{\psi}_q(z)\right]\\&\quad+\left[\mathbf{R}_n(\lambda_p a,\ z)\right]^T\mathbf{J}\left[\mathbf{R}_n(\lambda_q a,\ z)\right],\end{aligned}\tag{B1}$$

and

$$\left[\mathbf{K}_n(\lambda_p r)\boldsymbol{\psi}_p(z)\right]^T\mathbf{J}\left[\mathbf{K}_n(\lambda_q r)\boldsymbol{\psi}_q(z)\right]=\boldsymbol{\psi}_p^T\begin{bmatrix}\nu_{1n}&0&0&0&0&0\\0&0&0&0&0&0\\0&0&K_n&0&0&0\\0&0&0&K_n&0&0\\0&0&0&0&0&0\\0&0&0&0&0&\nu_{1n}\end{bmatrix}\mathbf{J}\begin{bmatrix}\nu_{1n}&0&0&0&0&0\\0&0&0&0&0&0\\0&0&K_n&0&0&0\\0&0&0&K_n&0&0\\0&0&0&0&0&0\\0&0&0&0&0&\nu_{1n}\end{bmatrix}\boldsymbol{\psi}_q$$

$$=rK_n\,\nu_{1n}(\boldsymbol{\psi}_p^T\mathbf{J}\boldsymbol{\psi}_q),\tag{B2}$$

$$\left[\mathbf{K}_n(\lambda_p r)\boldsymbol{\psi}_p(z)\right]^T\mathbf{J}\left[\mathbf{R}_n(\lambda_q r,\ z)\right]=\boldsymbol{\psi}_p^T\begin{bmatrix}\nu_{1n}&0&0&0&0&0\\0&0&0&0&0&0\\0&0&K_n&0&0&0\\0&0&0&K_n&0&0\\0&0&0&0&0&0\\0&0&0&0&0&\nu_{1n}\end{bmatrix}\mathbf{J}\begin{bmatrix}0&0&0&0&0&0\\0&-\upsilon_{1n}&0&0&0&0\\0&0&0&0&0&0\\0&0&0&\nu_{4n}&0&0\\0&0&0&0&-\upsilon_{4n}&0\\0&0&0&0&0&0\end{bmatrix}\begin{bmatrix}0\\1\\0\\1\\1\\0\end{bmatrix}\psi_{1q}$$

$$=\nu_{1n}\nu_{4n}\psi_{1p}\psi_{1q},\tag{B3}$$

$$\left[\mathbf{R}_n(\lambda_p r,\ z)\right]^T\mathbf{J}\left[\mathbf{K}_n(\lambda_q r)\boldsymbol{\psi}_q(z)\right]=\psi_{1p}(z)\begin{bmatrix}0\\1\\0\\1\\1\\0\end{bmatrix}^T\begin{bmatrix}0&0&0&0&0&0\\0&-\upsilon_{1n}&0&0&0&0\\0&0&0&0&0&0\\0&0&0&\nu_{4n}&0&0\\0&0&0&0&-\upsilon_{4n}&0\\0&0&0&0&0&0\end{bmatrix}\mathbf{J}\begin{bmatrix}\nu_{1n}&0&0&0&0&0\\0&0&0&0&0&0\\0&0&K_n&0&0&0\\0&0&0&K_n&0&0\\0&0&0&0&0&0\\0&0&0&0&0&\nu_{1n}\end{bmatrix}\boldsymbol{\psi}_q$$

$$=-\nu_{1n}\nu_{4n}\psi_{1p}\psi_{1q},\tag{B4}$$

$$\left[\mathbf{R}_n(\lambda_p r,\ z)\right]^T\mathbf{J}\left[\mathbf{R}_n(\lambda_q r,\ z)\right]=\psi_{1p}\begin{bmatrix}0\\1\\0\\1\\1\\0\end{bmatrix}^T\begin{bmatrix}0&0&0&0&0&0\\0&-\upsilon_{1n}&0&0&0&0\\0&0&0&0&0&0\\0&0&0&\nu_{4n}&0&0\\0&0&0&0&-\upsilon_{4n}&0\\0&0&0&0&0&0\end{bmatrix}\mathbf{J}\begin{bmatrix}0&0&0&0&0&0\\0&-\upsilon_{1n}&0&0&0&0\\0&0&0&0&0&0\\0&0&0&\nu_{4n}&0&0\\0&0&0&0&-\upsilon_{4n}&0\\0&0&0&0&0&0\end{bmatrix}\begin{bmatrix}0\\1\\0\\1\\1\\0\end{bmatrix}\psi_{1q}$$

$$=(\upsilon_{1n}\upsilon_{4n}-\upsilon_{1n}\upsilon_{4n})\psi_{1p}\psi_{1q}=0,\tag{B5}$$

https://doi.org/10.1017/jmech.2014.48 Published online by Cambridge University Press

then Eq. (B1) can be reduced to

$$(\mathbf{X}_{np})_{r=a}^{T}\mathbf{J}(\mathbf{X}_{nq})_{r=a} = rK_n\nu_{1n}(\boldsymbol{\psi}_p^T\mathbf{J}\boldsymbol{\psi}_q) + \nu_{1n}\nu_{4n}\psi_{1p}\psi_{1q} - \nu_{1n}\nu_{4n}\psi_{1p}\psi_{1q} = rK_n\nu_{1n}(\boldsymbol{\psi}_p^T\mathbf{J}\boldsymbol{\psi}_q)\,. \tag{B6}$$

So in Eq. (71), the expression

$$\int_{-h}^{h}(\mathbf{X}_{2p})_{r=a}^{T}\mathbf{J}(\mathbf{X}_{2q})_{r=a}\,dz = rK_2\nu_{12}\int_{-h}^{h}\boldsymbol{\psi}_p^T\mathbf{J}\boldsymbol{\psi}_q dz\,, \tag{B7}$$

possesses the symplectic orthogonality relation given by Eqs. (67).

REFERENCES

1. Timoshenko, S. P. and Goodier, J. N., *Theory of Elasticity*, 3rd Ed., McGraw-Hill, New York (1970).
2. Lekhnitskii, S. G., *Theory of Elasticity of an Anisotropic Body*, Mir, Moscow (1981).
3. Kotousov, A. and Wang, C. H, "Three-Dimensional Stress Constraint in an Elastic Plate with a Notch," *International Journal of Solids and Structures*, **39**, pp. 4311–4326 (2002).
4. Li, Z. H., Guo, W. L. and Kuang, Z. B., "Three-dimensional Elastic Stress Fields Near Notches in Finite Thickness Plates," *International Journal of Solids and Structures*, **37**, pp. 7617–7631 (2000).
5. She, C. M. and Guo, W. L., "Three-dimensional Stress Concentrations at Elliptic holes in Elastic Isotropic Plates Subjected to Tensile Stress," *International Journal of Fatigue*, **29**, pp. 330–335 (2007).
6. Yang, Z., Kim, C. B., Cho, C. and Beom, H. G., "The Concentration of Stress and Strain in Finite Thickness Elastic Plate Containing a Circular Hole," *International Journal of Solids and Structures*, **45**, pp. 713–731 (2008).
7. Folias, E. S. and Wang, J. J., "On the Three-dimensional Stress Field Around a Circular Hole in a Plate of Arbitrary Thickness," *Computational Mechanics*, **6**, pp. 379–391 (1990).
8. Folias, E. S., "On the Three-dimensional Theory of Cracked Plates," *Journal of Applied Mechanics*, **42**, pp. 663–674 (1975).
9. Kantorovich, L. V. and Krylov, V. I., *Approximate Methods of Higher Analysis*, Nordhoff, Groninger, the Nederlands (1964).
10. Tarn, J. Q., "A State Space Formalism for Anisotropic Elasticity, Part II: Cylindrical Anisotropy," *International Journal of Solids and Structures*, **39**, pp. 5157–5172 (2002).
11. Tarn, J. Q., Tseng, W. D. and Chang, H. H., "A Circular Elastic Cylinder under its Own Weight," *International Journal of Solids and Structures*, **46**, pp. 2886–2896 (2009).
12. Tarn, J. Q., Chang, H. H. and Tseng, W. D., "Axisymmetric Deformation of a Transversely Isotropic Cylindrical Body: A Hamiltonian State-space Approach," *Journal of Elasticity*, **97**, pp. 131–154 (2009).
13. Tarn, J. Q., Chang, H. H. and Tseng, W. D., "A Hamiltonian State Space Approach for 3D Analysis of Circular Cantilevers," *Journal of Elasticity*, **101**, pp. 207–237 (2010).
14. Tarn, J. Q. and Tseng, W. D., "Exact Analysis of Curved Beams and Arches with Arbitrary End Conditions: A Hamiltonian State Space Approach," *Journal of Elasticity*, **107**, pp. 39–63 (2012).
15. Hildebrand, F. B., *Advanced Calculus for Applications*, 2nd Ed., Prentice-Hall, Englewood Cliffs, New Jersey (1976).
16. Zhong, W. X., *A New Systematic Methodology for Theory of Elasticity*, Dalian University of Technology Press, Dalian, China (1995). (in Chinese).

(Manuscript received September 7, 2013,
accepted for publication March 3, 2014.)

https://doi.org/10.1017/jmech.2014.48 Published online by Cambridge University Press